Detecting and Locating of Brain Abnormality in MR Images Using Texture Feature Analysis and Improved Probabilistic Relaxation Methods

YAO-MING YU
Institute of Computer and Communication Engineering
National Taipei University of Technology, Taiwan
1, Sec. 3, Chung-hsiao E. Rd., Taipei, 10608, Taiwan, R.O.C.
wtjacky@ms68.hinet.net

Abstract: - Medical imaging has become a major tool in clinical trials since it enables rapid diagnosis with visualization and quantitative assessment. In the study, a detecting method of brain abnormality is proposed through magnetic resonance imaging. The proposed method is composed of four procedures. First the preprocessing is employed to remove noises and enhance the homogeneity of soft tissues. After preprocessing, we adopt the spatial gray level dependence method to compute four texture features of each image. Then, the improved probability relaxation method is applied to discriminate the brain abnormality with extracted texture information. The isolated noises are removed by using neighborhood processing. Final the performance of the improved method has been evaluated and compared to the original method. This proposed method performs better results than the other one, which can be used in further processing stages. We have developed a computer-aided detection system to distinguish the tumor and find the location and coarse contour from brain MRIs. The system can assist doctors to diagnose whether the brain has abnormal and train inexperienced doctors. The proposed algorithm can play a useful role for storage, filtering and indexing of mass MRI data, and furthermore it provides an initial step to find accurate tumor boundaries.

Key-Words: - Computer-Aided Detection System, Texture Feature Analysis, Spatial Gray Level Dependence, Probability Relaxation Method, Magnetic Resonance Image, Brain Tumor

1 Introduction

The average adult human body is made up of 10-50 trillion cells. Each cell has specific duty. The cells growth in the body and are divided to reproduce other cells. These divisions are very vital for correct functions of the body. When each cell loses the ability of controlling its growth, these divisions are done with any limitation and tumor emerges. Tumors, their self, are divided to tow classes: benign and malignant [1]. A tumor is a mass of tissue that grows out of control of the normal forces that regulate growth [2]. Brain tumors are abnormal growths or masses in the brain. Primary brain cancers arise directly from the cells of the brain. They can be noncancerous or cancerous. Brain tumor is one of the major causes for the increase in mortality among children and adults. The Central Brain Tumor Registry of the United States (CBTRUS) estimates the occurrence of approximately 63,000 new cases of brain and nervous system tumors among Americans in 2010. Roughly one-third of primary brain and central nervous system tumors are cancerous. In addition to primary brain tumors, cancers from other parts of the body can spread to the brain and cause tumors. These tumors are called metastatic or secondary brain tumors. Metastatic brain tumors are more common than primary brain tumors, especially among adults.

Medical imaging has become a major tool in clinical trials since it enables rapid diagnosis with visualization and quantitative assessment. It is divided to anatomical and physiological. The anatomical imaging includes mainly computer tomography (CT), ultrasound, and magnetic resonance imaging (MRI). MRI is primarily a medical imaging technique most commonly used in radiology to visualize the structure and function of the body. It provides much greater contrast between the different soft tissues of the body than does CT, making it especially useful in neurological (brain), musculoskeletal, and oenological (cancer) imaging [3]. Besides, the advantages of MRI over other diagnostic imaging modalities are its high spatial resolution and excellent discrimination of soft tissues. It provides rich information about

anatomical structure, enabling quantitative pathological or clinical studies [4]; the derivation of computerized anatomical atlases [5]; as well as pre and intra-operative guidance for therapeutic intervention [6, 7]. Such information is also valuable as an anatomical reference for functional modalities, for example positron emission tomography (PET) [8], single photon emission computerized tomography (SPECT), and functional MRI [9].

Computer science is prosperous recently. Computer digital image is more progressive in software and hardware, so it is extensively used to diagnose many kinds of diseases. It not only assists doctors to diagnose, but also use it to train inexperienced doctors. It makes diagnosis more correct and speedy. So in the study, we developed Computer-Aided Detection (CAD) system for detection of brain abnormality through MRI. The organization of paper is as follows. At next section, paper introduces about the experimental procedures that are divided to image preprocessing, texture feature extraction, brain abnormality discrimination, and final process. These procedures have been respectively explained about details in each subsection. At result section, some experimental results are shown. The discussion section explains the applications, features, and limitations of this work. Finally, we describe some other future works in the conclusion section.

2 Material and Methods

In the study, we developed detection and location system of brain abnormality through MRI. For achieving the goal, the proposed system is consisted of four procedures, including the image preprocessing for noise reduction and image enhancement in MRIs, the texture feature extraction using spatial gray level dependence (SGLD), the brain abnormality discrimination by the symmetry of brain with improved probability relaxation method (IPRM), and the final stage for removal isolated noise using neighborhood processing. Each algorithm has been introduced about details as follows.

2.1 Image Preprocessing

Image preprocessing is an essential procedure and the simplest categories of medical image processing. This stage is used for reducing image noise, highlighting edges, or displaying digital images. These are used to suppress noise and imaging of spectral parameters. After this stage the medical image is converted into standard image without noise, film artifacts, or labels. Preprocessing techniques are used to improve the detection of the suspicious regions in MRI. In the work, the preprocessing method consists of three steps: first, the negative of an image with gray levels is obtained by using the negative transformation. Second, a 3×3 median filter is used to reduce noise. Finally, image equalization is applied to smooth the gray level image with an average value.

2.2 Spatial Gray Level Dependence

The features are different between normal and abnormal in region of interest (ROI) for brain MRIs. In general, the intensity of tumor region is higher than the surrounding normal tissue. The other texture features are also diverse, such as contrast, entropy, homogeneity, and so on. It is useful information when these features are utilized to distinguish the tumor from the other normal tissues. A doctor can determine the diseases based on his experience and the characteristics of the patient's MR images. In the study, we quantify the property of these texture features specifically. Two types of statistical equation are adopted. One is used to compute the first-order parameters as shown in Eqs. (1) - (2); the other is used to compute second-order parameters as shown in Eqs. (3) - (4). The second-order parameters originally can be derived from a second-order joint probability by using the spatial gray level dependence (SGLD) method. Then, all the calculated parameters can represent texture features of the specific ROI. Using the parameters, the region of image that contains the weight group of statistical parameters can be described.

First-Order parameters:

$$Mean = \frac{1}{N}\sum_{ij} g(i, j) \tag{1}$$

$$Variance = \frac{1}{N}\sum_{ij} (g(i, j) - Mean)^2 \tag{2}$$

where $g(i, j)$ is the gray level of pixel coordinated with (i, j) and N is the number of pixels in ROI.

Second-Order parameters:

$$Inertia(P_\theta(\delta)) = \sum_{i=0}^{L-1}\sum_{j-0}^{L-1}(P_\theta(i,j\mid\delta)(i-j)^2) \quad (3)$$

$$Entropy(P_\theta(\delta)) = -\sum_{i=0}^{L-1}\sum_{j=0}^{L-1}P_\theta(i,j\mid\delta)\log P_\theta(i,j\mid\delta) \quad (4)$$

where $p(i,j\mid\delta,\theta)$ is a second-order joint probability and based on the spatial gray-level co-occurrence matrix of an image.

The spatial gray level dependence has been widely used for texture analysis. It is often used to analyze the different feature of tissues according to viewpoint of the research. The method is based on the estimation of the second-order joint conditional probability density function, $p(i,j\mid\delta,\theta)$. The $p(i,j\mid\delta,\theta)$ is the probability from gray level i to gray level j in the given inter-sample spacing δ and direction angle θ. The estimated values can be written as a gray-level co-occurrence matrix that is extensively used in texture analysis [10]. The normalized gray-level co-occurrence matrix is defined as:

$$P(i,j\mid\delta,\theta) = T(i,j)\Big/\sum_{i=1}^{L}\sum_{j=1}^{L}T(i,j) \quad (5)$$

where $T(i,j)$ represents the times of texture change from gray value i to j in (δ,θ) condition , and L represents the gray level number of the image.

According to Eq. (5), the normalized gray-level co-occurrence matrix can be calculated. The entries of the normalized $P(i,j\mid\delta,\theta)$ are limited from 0 to 1. The gray-level co-occurrence matrix intrinsically reflects one kind of statistical texture properties. The method is called texture statistics or texture measurement.

2.3 Improved Probabilistic Relaxation Method

For understanding image, context of the image acts an important role. To analyze the context of image, first let the given image be divided into several subimages called regions. Two sets of regions belong to two images, respectively. The inter-relationships are described by an adjacency region. A binary relaxation algorithm determines the inter-relationship between the two regions. Then, each binary relationship is assigned to a label value. From the assigned label value, the relationship of two images can be understood. Usually, the labels are assigned by two main methods that include discrete and probabilistic labeling.

In this study, we also propose an improved relaxation labeling method. The method is based on the original probabilistic relaxation method [11]. In order to suitably discriminate the abnormality from brain MR images, the original method is modified. The improved probability relation method (iPRM) is more appropriate for the subject and object of experiment with four texture features. There are a series of definitions as follows for the presented method:

1. As an illustration in Fig. 1, we define the initial no-contextual probability formula using Eq. (6).

$$P^0(\theta_i = l_j) = 1 - \left\{\sum_{k=1}^{4}\left(T_{i,k} - T_{j,k}\right)^2\right\}^{\frac{1}{2}} \Big/ \sum_{j=1}^{9}\left\{\sum_{k=1}^{4}\left(T_{i,k} - T_{j,k}\right)^2\right\}^{\frac{1}{2}} \quad (6)$$

where T is texture parameter value for each subimage, k is number of texture parameter for each subimage.

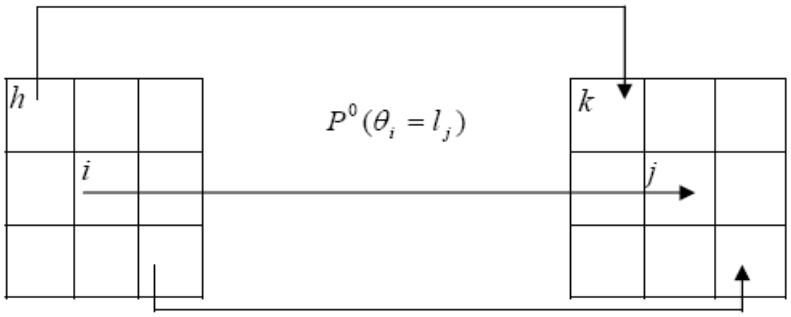

Fig. 1. Define initial no-contextual probabilities of labels for each pair of subimages (u_i, u_j) that belong to abnormal and normal images, respectively.

2. As illustrated in Fig. 2, we define the q^r support of the unit u_i whose label θ_i will be assigned to l_j resulting from all N-1 directly interact other units u_j at the r^{th}. Note that the k is in range 3.

$$q^r(\theta_i = l_j) = \frac{1}{N-1}\sum_{\substack{h=1 \\ \neq i}}^{N}\sum_{k=1}^{3} C_k(\theta_i = l_j, \theta_h = l_k) P^r(\theta_h = l_k) \quad (7)$$

where compatibility coefficient C_k is defined as follows:

$$C_1 = \frac{P^r(\theta_h = l_{k_1})}{P^r(\theta_i = l_j)} \quad (8)$$

$$C_2 = \begin{cases} \dfrac{P^r(\theta_h = l_{k_2})}{P^r(\theta_i = l_j)} + 1 & \dfrac{P^r(\theta_h = l_{k_2})}{P^r(\theta_i = \theta_j)} \geq threshold \\ \dfrac{P^r(\theta_h = l_{k_2})}{P^r(\theta_i = l_j)} - 1 & otherwise, \end{cases} \quad (9)$$

$$C_3 = \frac{P^r(\theta_h = l_{k_3})}{P^r(\theta_i = \theta_j)} \quad (10)$$

Note that, each only unit u_h only interacts with these units, such as k_1, k_2, and k_3.

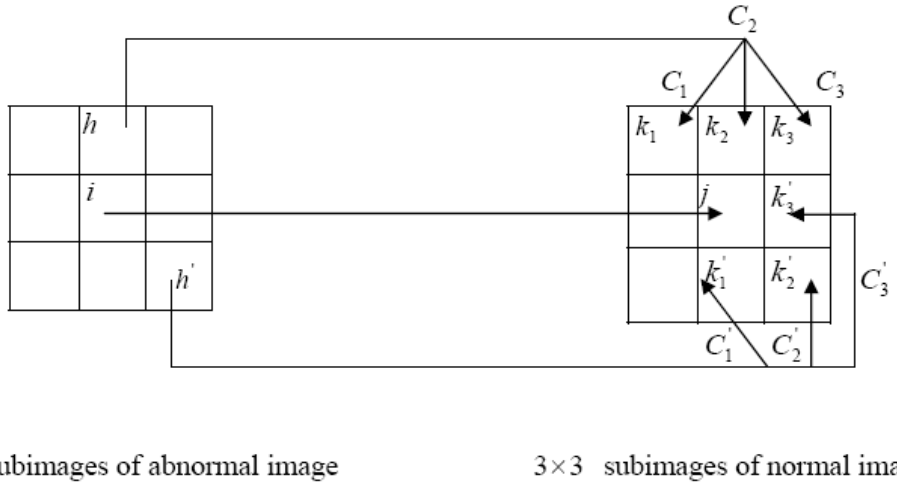

Fig. 2. Define the support q^r of Eq. 7 for each pair of subimages that belong to abnormal and normal images, respectively.

3. An updating iterative formula is given, which specified the new probability $P^{r+1}(\theta_i = l_j)$ of

a label θ_i according to the previous probability $P^r(\theta_i = l_j)$ and probabilities of labels of all supportive interacting units,

$$P^{r+1}(\theta_i = l_j) = \frac{1}{Q} P^r(\theta_i = l_j)(1 + q^r(\theta_i = l_j)) \quad (11)$$

where Q is a normalizing constant with

$$Q = \sum_{j}^{M} P^r(1 + q^r(\theta_i = l_j)) \text{ and } P^0(\theta_h = l_k) \quad (12)$$

Then, the algorithm of improved probabilistic relaxation labeling can be depicted in the following steps:

Step 1. Define initial conditional probabilities of labels for all units u_i in the image using Eq. (6).

Step 2. Compute the convergent function, which represents the quality of the image labeling.

Step 3. Minimize the value of the convergent function by updating probabilities of unit label using Eqs. (7) through (12).

Step 4. Repeat steps 2 and 3 until the minimal value of the convergent function is reached.

2.4 Final process

After a sample image is processed using the improved probability relaxation, we can get the preliminary result. In order to reduce isolated noise point, we use neighborhood operation of filtering processing to solve this question. A sliding neighborhood operation is performed a pixel at one time, with the value of any given pixel in the output image being determined by the application of an algorithm to the values of the corresponding input pixel's neighborhood. A pixel's neighborhood is some set of pixels, defined by their locations relative to that pixel, which is called the center pixel. The neighborhood is a rectangular block, and as you move from one element to the next in an image matrix, the neighborhood block slides in the same direction. In the work, we use algorithm of four neighbors in image processing to reduce isolated noise point. After computing of four neighbors, we chose a maximum area which will be possible area of brain tumor.

3 Results

3.1 Texture Feature Analysis

After image preprocessing, many unnecessary noises disappear but similar properties of brain tumors also increase. The important goal of next step, we will detect whether the abnormality exist in brain MRIs or not. It is good method to use SGLD to get features information of brain MRIs. Due to the coarse degree and distributive state of gray level are enormous differences between abnormality and normal tissues. So feature analysis of tumor boundary is added to improve efficiency of identifying system. The SGLD method is relation to property of structure in regions. Therefore it is very important to decide the size of subimage which we will analyze. Too small subimage cannot find obviously difference between tumor and normal tissue, and too large subimage makes decision indistinct. The optimum size of each subimage is 8×8 pixels by experiment. After SGLD processing, the result can be regarded as a piece of feature image. In the work, four features of tissue: *Inertia*, *Entropy*, *Mean*, *Variance* would be solved by using SGLD method, so the results of one image can be regarded as small four pieces of feature image.

We understand that co-occurrence matrix need to be solved first before processing SGLD method. In this study, the sample distance δ in co-occurrence matrix is set as 1 and the sample angle θ is set as 0^0 and 90^0, so the opposite pixel of pixel (i, j) in co-occurrence matrix is $(i+1, j+1)$ and $(i+1, j-1)$, the relative probability of gray level value between each pixels and its opposite pixels in co-occurrence matrix is recorded by co-occurrence in subimages. It is not easy to obtain the normal and healthy MRI after a people maybe become ill. Owing to the texture features of abnormal region are distinct from the normal tissue so we apply the other half brain of without tumor to automatically reflect a complete and normal MRI by using the principle of brain symmetry. A sample of brain abnormality is shown in Fig. 4 (A). The sample MRI is divided equally, as shown in Fig. 4 (B). The normal MRI is simulated and depicted in Fig. 4 (C) by using the principle of brain symmetry.

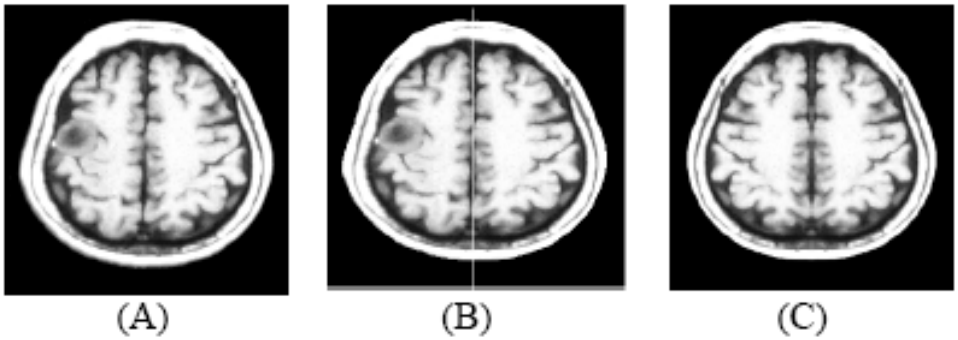

Fig. 4. Using the principle of brain symmetry simulates a complete and normal MRI. (A) A sample of brain abnormality. (B) Cut the sample MRI equally. (C) The simulated and normal MRI.

The images of normal and abnormality are partitioned into many blocks before the analysis of texture feature respectively. Each block of the abnormal and normal MRI consists of 30 subimages, as shown in Fig. 5. Then, we calculate four texture features of each subimage below.

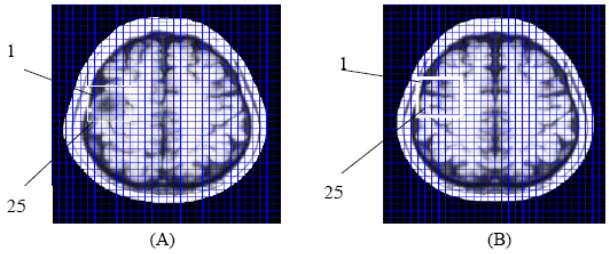

Fig. 5. Every block of the abnormal and normal MRI is divided into 30 subimages. (A) displays the abnormal brain MRI; (B) illustrates the normal brain MRI.

3.2 Abnormality Discrimination

According to the symmetry of brain organ and texture feature analysis, we get the difference of features between abnormal and normal tissue. After the texture feature analysis of abnormal and normal image, each subimage has four texture parameters. Every captured feature by texture feature analysis must be appropriate to represent the property of the MRI. Then, the improved probability relaxation method is employed to process texture features and extract the position of brain tumor. The relative probability value of each pair of subimages can be identified between normal and abnormal image. If two subimages are similar, the probability value approaches to 1. Inversely, the probability value approaches to 0. From the results of experiment, the position of tumor can be detected in the abnormal brain MRI. A sample of abnormal brain MRI is processed using the improved probability relaxation; we get the relaxation result, as shown in Fig. 6. Observing the Fig. 6 (C), the white blocks represent the possible and candidate region of brain abnormality; the black areas illustrate the background and normal region. The iPRM is more appropriate and effective for distinguishing the abnormality from brain MRI with four texture features.

We observe from the experimental result that there are many unnecessary and questionable regions. In order to reduce isolated noise points, we use neighborhood operation of filtering processing to solve this question after analyzing the Fig. 6 (C). We chose a maximum area which will be the most possible area of brain tumor after computing of four neighbors, as shown in Fig. 7 (C). Through the procedure of final process, we can find the coarse contour of brain tumor. For observing and comparing the different results of experiment under the same preparation and process, the other abnormal brain MRI is taken as the second sample and goes through the same procedure of implement. The final result is depicted in Fig. 8.

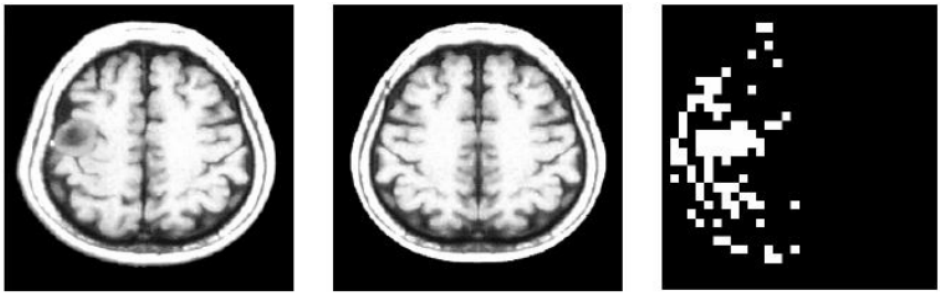

Fig. 6. The relaxation result of an abnormal brain MRI. (A) a sample of abnormal MRI, (B) simulated and normal MRI, (C) the relaxation result. Note that normal MR image is created from the right half part of (A).

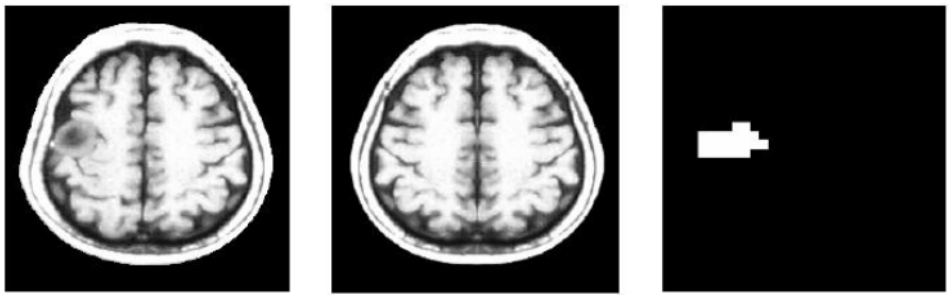

Fig. 7. The experimental result of the first sample using the proposed procedure. (A) abnormal brain MRI, (B) simulated and normal brain MRI, (C) the region of tumor candidate.

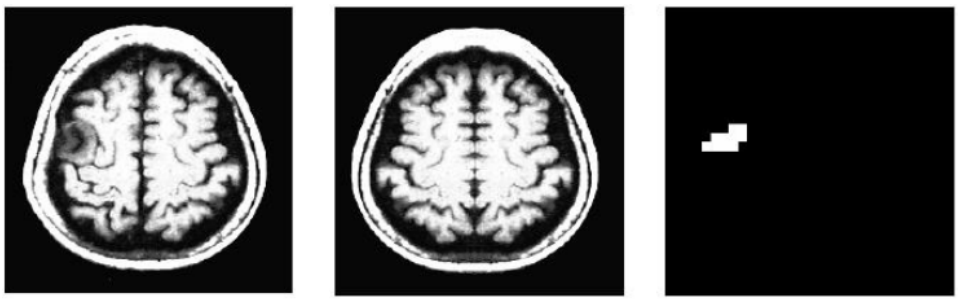

Fig. 8. The other sample goes through the same procedure of implement. (A) abnormal brain MRI, (B) simulated and normal brain MRI, (C) the region of tumor candidate.

4 Discussion

Texture features belong to one of photometric features that are derived directly from raw pixel intensities. These encode spatial organization of pixel values of an image region. The common practice to obtain texture-based descriptors is to invoke standard transform domain analysis tools such as Fourier transform, wavelets, Gabor, or Stockwell filters on local image blocks [13-16]. Besides, a series of commonly used texture measures (derived from the Grey Level Co-occurrence Matrix, GLCM) also called Haralick's texture features are available. These texture features can be derived from a local image neighborhood such as energy, entropy, coarseness, homogeneity, contrast, etc. [15-16] or utilize linear system approaches such as simultaneous autoregressive models. In the study, we apply the SGLD to extract features in characterizing abnormality. These features are used by not only considering the

distribution of gray level, but also presenting an accurate second-order description of varying gray level caused by textures.

We utilize the proposed method to detect whether the abnormality exist in brain MRIs or not and find the location and region of brain abnormality. In order to get the qualified experimental results, it is critical and noteworthy to decide the size of subimage when we process the SGLD method to extract the texture features from brain MRIs. Due to the SGLD is relation to the property of structure in regions. Therefore it is very important. Too small subimage cannot find obviously difference between normal tissue and abnormal region, and too large subimage makes decision indistinct. In addition, the feature selection is also crucial to the segmentation of an image such as energy, coarseness, homogeneity, contrast, and so on.

The performance of the proposed algorithm has been evaluated and compared to the original method. To evaluate the practical performance of the improved method, the algorithm has been implemented in Matlab7.0 under window XP system. The few images are given below to know how the medical image locating is taken place. In Fig. 9 (A) indicates the MR medical images, (B) displays the experimental results using PRM method, and (C) exhibits the consequences using improved method. Quantitative comparisons of both techniques can be found in Table 1, which gives the computational time and the size of candidate area. The size of each subimage is 8×8 pixels. We observed that the performance of improved method is better than original method from Fig. 9 and Table 1.

This study has several limitations. First, the experimental result will be influenced if the status of brain symmetry is unobvious. The second limitation of the study, the tumor cannot be detected when the size of tumor is too small. The unapparent tumor will be neglected after the neighborhood operation is performed. Third, the MR image can’t be processed when left and right half-brain have abnormal simultaneously.

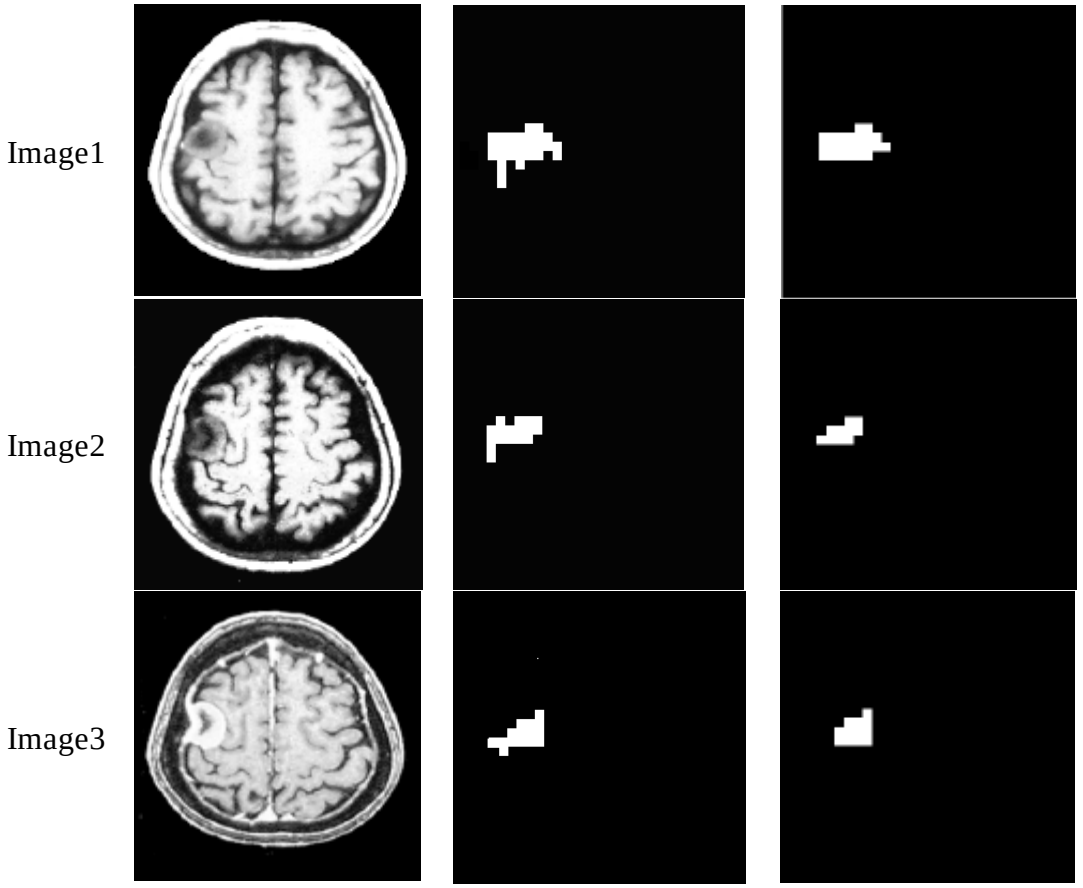

Fig. 9. A comparison between the original and improved method for detecting and locating of brain abnormality in three different MR images.

Table 1. Quantitative comparisons

S. No	Original method		Improved method	
	Computational Time (seconds)	Subimage Number	Computational Time (seconds)	Subimage Number
Image1	1.32	28	1.17	23
Image2	1.15	15	0.97	11
Image3	1.28	15	1.04	12

5 Conclusions

The image process is extensively used in many kinds of diagnosing diseases. MRI has more convenient, correct and high-quality in checking the abnormality of tumor. In the study, we have developed an effective detecting system to distinguish the tumor from brain MRIs and to find the location and coarse contour of brain tumor by the proposed algorithm. Observing the shape of original MRI, the message is very limited. Sometimes, the brain image may be too complicated or small in tissue to accurate observe by human eyes. Due to computer assisting, the position and shape of brain abnormality may be detected accurately and can avoid missing out the brain tumor.

In this study, first preprocessing is employed to remove the noise and inhomogeneous soft tissues, and then the SGLD method is used to extract four texture features from brain MRIs. After this, we adopt the improved probability relaxation method to find the location of brain tumor. The proposed methods can distinguish if there are

abnormalities in brain MRIs. Following this, the coarse contour of brain abnormality can be found to help the disease diagnosis. Our approach utilizes approximate left-right symmetry of the brain. It does not require image registration. Only four extracted texture features and un-complex methods are used. This study can play a useful role for storage, filtering and indexing of mass MRI data, and furthermore it provides an initial step to find accurate tumor boundaries.

Due to the characteristic of brain tumor is complex, doctors not only need to depend on their experiences but also need the assistant system to promote the diagnosis accuracy. So, it is very important and valuable to detect the accurate region of brain tumor and differentiate the classification of tumor. Furthermore, the 3D reconstruction of image is very useful for the diagnosis and treatment of lesions. The 3D image is beneficial to the tumor detecting, clinical diagnosis, and training education. Therefore we want to develop a whole classification system of 3D brain tumors in the future.

Acknowledgement

The authors would like to thank Dr. Yung-Hsiao Chiang, Dr. Shinn-Zong Lin of the Department of Neurological Surgery, Tri-Service General Hospital, Taiwan, for their continuous support during the project.

References

[1] A.E. Lashkari, A Neural Network based Method for Brain Abnormality Detection in MR Images Using Gabor Wavelets, *International Journal of Computer Applications*, Vol.4, No.7, July 2010, pp. 9-15.

[2] P. Lin, Y. Yang, C.X. Zheng, J.W. Gu, An Efficient Automatic Framework for Segmentation of MRI Brain Image, *Proceedings of the Fourth International Conference on Computer and Information Technology(CIT'04)*, IEEE, 2004.

[3] H.B. Kekre, S. Gharge, Direct Variance on MRI Images for Tumor Detection, *Journal of Sci., Engg. & Tech. Mgt.*, Vo1.2, No.1, January 2010, pp.3-11.

[4] M. Shenton, R. Kikinis, F. Jolesz, et al., Abnormalities of the Left Temporal Lobe and Thought Disorder in Schizophrenia, *N. Engl. J. Med.*, Vol. 327, No.9, 1992, pp. 604-612.

[5] K. Hohne, et al., A framework for the Generation of 3D Anatomical Atlases, *SPIE, Visualization in Biomedical Computing*, Vol. 1808, 1992, pp. 169-213.

[6] R. Kikinis, F.A. Jolesz, W.E. Lorensen, H.E. Cline, P.E. Stieg, Black 3d Reconstruction of Skull Base Tumors from MRI Data for Neurosurgical Planning, *In Proceedings of the Society of Magnetic Resonance in Medicine Conference*, 1991.

[7] R. Kikinis, D. Altobelli, W. Lorensen, W. Wells, G. Ettinger, Pre- and intraoperative tumor localization using 3d renderings of MRIs, *12th Annual Scientific Meeting of the Society of Magnetic Resonance in Medecine*, 1993.

[8] D. Levin, X. Hu, K. Tan, et al., The Brain: Integrated Three-Dimensional Display of MR and PET Images, *Radiology*, Vol. 172, No.3, 1989, pp. 783-789.

[9] J. Belliveau, D. Kennedy, R. McKinstry, et al., Functional Mapping of the Human Visual Cortex by Magnetic Resonance Imaging, *Science*, Vol.254, No.5032, November 1991, pp. 716-719.

[10] A.H. Mir, M. Hanmandlu, S.N. Tandon, Texture Analysis of CT Images, *IEEE Engineering in Medicine and Biology*, Vol.14, No.6, 1995, pp. 781-786.

[11] A. Rosenfeld, R. Hummel, S. Zucker, Scene labeling by relaxation algorithms, *IEEE Trans. Syst., Man, Cybern.*, Vol. 6, 1976, pp. 420-433.

[12] M. Sonka, V. Hlavac, R. Boyle, Image Processing, Analysis, and Machine Vision, *Thomson*, New York: Brooks, 2008.

[13] D.M. Kwak, B.S. Kim, O.K. Yoon, C.H. Park, J.U. Won, K.H. Park, Content-Based Ultrasound Image Retrieval Using a Coarse to Fine Approach, *Annals of the New York Academy of Sciences*, Vol.980, 2002, pp. 212-224.

[14] J. Lim, J.P. Chevallet, A visual vocabulary approach for medical image indexing and retrieval, *In Second Asia Information Retrieval Symposium*, Jeju Island, Korea, 2005.

[15] S. Doyle, et al, Using manifold learning for content-based image retrieval of prostate histopathology, *In MICCAI 2007 Workshop on Content-Based Image Retrieval for Biomedical Image Archives*, Brisbane, Australia, 2007.

[16] M. Gletsos, et al, A computer-aided diagnostic system to characterize CT focal liver lesions: design and optimization of a neural network classifier, *IEEE Trans. Inf. Technol. Biomed.*, Vol.7, No.3, 2003, pp. 153–162.